

# A Triple-Band Compact Antenna Based on CSRR and LHTL

Jiaran Qi, Chang Liu, Shanshan Xiao

Dept. of Microwave Engineering, School of Electronics and Information Engineering  
Harbin Institute of Technology  
Harbin, China, 150086  
qi.jiaran@hit.edu.cn

**Abstract**—A triple-band compact antenna fed by coplanar waveguide (CPW) suitable for indoor communication is presented in this paper. The proposed structure is the combination of a complementary split-ring resonator (CSRR) and a left-handed transmission line (LHTL). The CSRR, working in quarter-wave monopole mode, contributes the first two operating frequency bands, which are further broadened by an additional triangular transitional structure. The LHTL implemented by interdigital capacitors and ground poles provides the third frequency band operating in a resonant mode. Detailed simulation results are presented to confirm our idea and design procedure.

**Keywords**—triple-band antenna; CSRR; LHTL; indoor communication

## I. INTRODUCTION

With the rapid development of modern wireless indoor communication, new requirements and meanwhile challenges have recently arisen for the corresponding antenna system. Among them, the question how to use one antenna to receive and transmit multiple signals of different frequencies has received more and more attention. As multi-band antennas have the advantages of flexibility, compactness in size, ease to carry, and low cost, they have been widely applied in various wireless communication systems. Recently, the design of multi-band antenna becomes more and more popular [1–6]. In [1], a dual-band circularly polarized antenna is achieved by double-sided printed and cross-shaped dipoles, where CSRRs are applied as two arms of the dipole antenna. Another dual-band asymmetric dipole antenna is achieved by adding an asymmetrically barbed arrowhead on each dipole arm for global positioning system (GPS) applications [2]. In [3], a triple-band linearly polarized patch antenna and a dual-band dually polarized patch antenna are proposed based on a modified mushroom unit cell. By loading on the planar dipole antenna composite right left handed (CRLH), a new dual/triple band metamaterial antenna is presented in [4]. Multi-band antennas are achieved by introducing multiple geometrical branches to the dipole arms in [5, 6]. The abovementioned antenna structures, however, display usually relatively narrow operating frequency bands. In addition, the radiation properties at a certain frequency band may deteriorate which limits the practical implementation of the proposed antenna. In this paper, a triple-band antenna based on CSRR and LHTL is

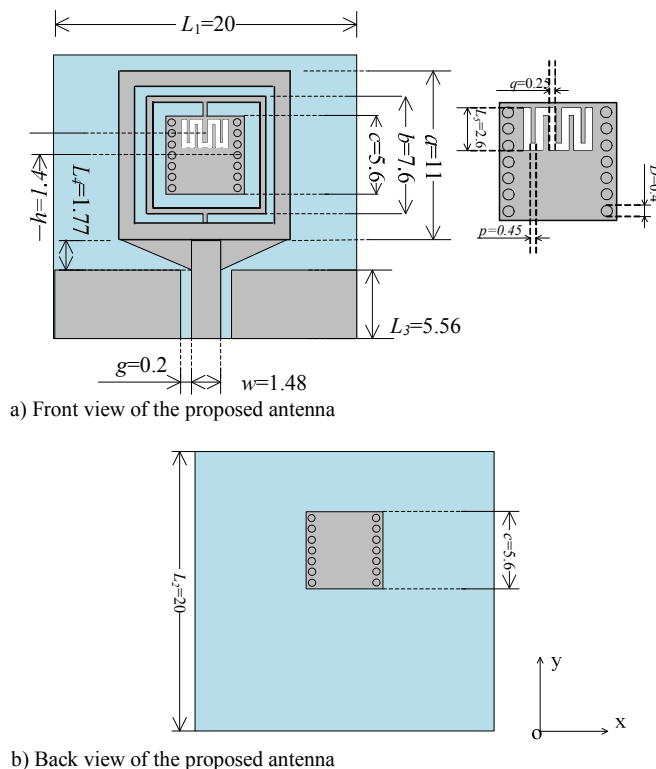


Fig. 1. Geometry of the proposed antenna. All units are in millimeters.  $L_1$  is the length of substrate.  $L_2$  is the width of substrate.  $a$  is the length of the outermost square strip.  $b$  is the length of the inner ring.  $c$  is the length of the square patch.  $L_3$  is the width of virtual ground.  $L_4$  is the height of triangular transitional element.  $g$  is the gap width between CPW and virtual ground.  $w$  is the feeding-strip width of CPW.  $h$  is the offset distance of interdigital structure from the center of the square patch.  $p$  is finger width.  $q$  is gap width.  $D$  is diameter of the metal post.  $L_5$  is the finger length.

proposed, which can operate at 3.95 GHz, 5.4 GHz and 7.4GHz with acceptable radiation properties. The proposed antenna configuration is elucidated. The operation modes of the proposed antenna at different frequency bands are explained, confirmed by detailed simulation results.

## II. ANTENNA CONFIGURATION

The geometry of the proposed antenna is illustrated in detail in Fig. 1. The planar antenna structure including CSRR, LHTL, CPW, triangular impedance matching elements, and

virtual ground, is etched on both sides of a  $20 \times 20 \times 0.8 \text{mm}^3$  substrate with relative permittivity  $\epsilon_r (=4.4)$ . On the front side of the substrate as shown in *Fig. 1(a)*, the CSRR strip is constructed by three concentric elements, i.e., two metallic square strips and one square patch. The length  $a$  of the outermost square strip is 11mm, and its width is 1mm. The length  $b$  of the inner ring is 7.6mm, and its width is 0.3mm. They are electrically connected via a short stub, forming one split-ring slot resonator (SRR). Another complementary SRR is formed by the inner square strip and the square patch of side length  $c (=5.6\text{mm})$ , electrically connected by another stub. The CSRR is then fed by CPW, whose geometric parameters are listed in *Fig. 1*. It should be mentioned that in order to broaden the impedance bandwidth of the CSRR-based monopole antenna two triangular transitional elements are inserted between the CSRR radiator and the CPW. Up to now, a dual band monopole antenna based on CSSR is complemented.

Furthermore, an interdigital capacitor [7], with finger width  $p (=0.45\text{mm})$ , gap width  $q (=0.25\text{mm})$ , and gap length  $L_5 (=2.6\text{mm})$ , is fabricated on the square patch to achieve the left-handed capacitor. In order to realize the LHTL, we firstly add on the backside of the substrate a square patch of side length  $c$  as the virtual ground, as shown in *Fig. 1(b)*. Then, via totally 14 metal posts of diameter  $D (=0.4\text{mm})$ , the upper and lower metallic square patches are electrically connected, realizing the left-handed inductor. Finally, a different radiation mechanism based on LHTL is successfully implemented to the original CSSR monopole antenna, leading to an additional frequency band without increasing the antenna dimension.

### III. SIMULATION RESULTS AND DISCUSSION

In this section, we will firstly demonstrate with simulation results the influence of several critical geometrical parameters on the operating frequency bands of the proposed antenna. Then, the simulated impedance and radiation properties of the antenna with the optimized geometry will be illustrated.

It has been pointed out previously in this paper that the CSRR-based antenna contributes the first two operating frequency bands, while the LHTL structure influences the third and highest frequency band. As shown in *Fig. 2*, the center frequency is around 4GHz when the length  $a$  of the outermost square strip is 9mm, approximately a quarter effective wavelength. Similarly, it can be observed in *Fig. 3* that the center frequency is around 5.8GHz when the length  $b$  of the inner square strip is 6.8mm, also around a quarter effective wavelength. Furthermore, *Fig. 2* shows that the length  $a$  of the outmost square strip has the most significant influence on the first and lowest operating frequency band. With the increasing  $a$ , the decreasing center frequency is observed. It is also illustrated in *Fig. 3* that the length  $b$  of the inner square strip has the most significant influence on the second operating frequency band. The corresponding center frequency is inversely related to  $b$ . It should thus be noted that the CSRR radiator shares similar characteristics to ordinary quarter-wave monopole antennas. The center frequency of the resulting frequency band is closely related to the arm length of the SRR. The simulated radiation pattern shown later in this paper will further confirm this point. In order to broaden the impedance bandwidth of the CSRR-based monopole antenna,

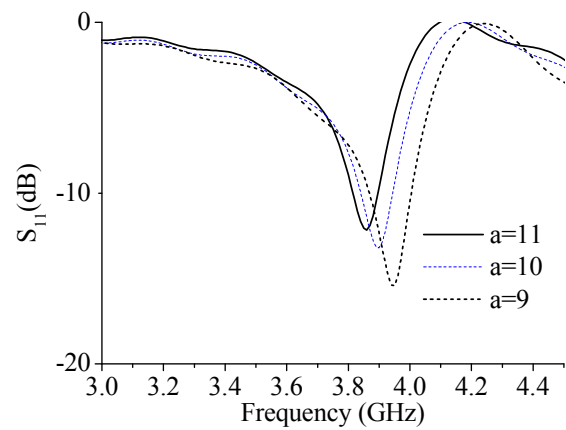


Fig. 2. The dependence of the return loss  $S_{11}$  on the length  $a$  of the outermost square strip

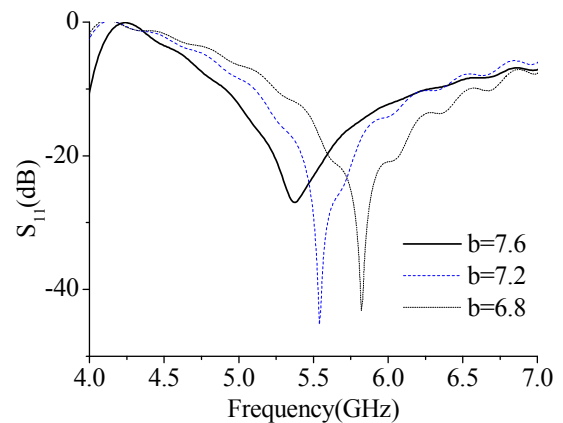


Fig. 3. The dependence of the return loss  $S_{11}$  on the length  $b$  of the inner square strip

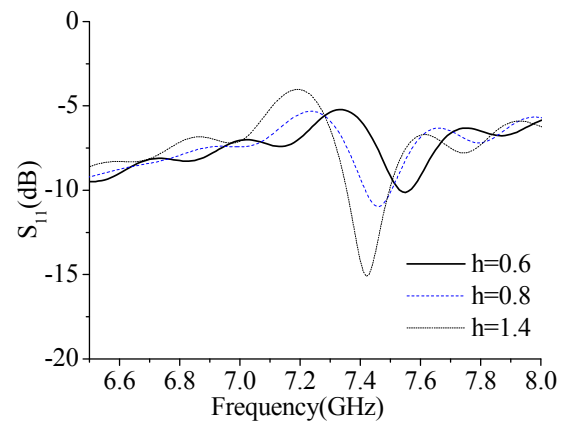


Fig. 4. The dependence of the return loss  $S_{11}$  on the offset distance  $h$  of the interdigital capacitor from the center of square patch

two triangular transitional elements as shown in *Fig. 1* are inserted between the CSRR radiator and the CPW.

Different from the CSRR-based elements, the additionally introduced LHTL structure operates in a different resonant mechanism. In order to realize a LHTL structure, the so-called left-handed capacitor and left-handed inductor have to be constructed. In this paper, we adopt an interdigital structure to

achieve the on-patch or left-handed capacitor, and grounded metal posts to obtain inter-patch or left-handed inductor. By optimizing the geometrical parameters of LHTL, i.e., finger width  $p$ , gap width  $q$ , and gap length  $L_5$ , we can achieve a third and higher frequency band at around 7.5GHz. It needs to be emphasized that the impedance matching can be greatly enhanced by adjusting the position of the on-patch interdigital capacitor. It can be seen from Fig. 4 that when the offset distance  $h$  of interdigital structure from the center of the square patch is increased, the  $-10$ dB bandwidth is improved.

Finally, simulated impedance bandwidth of the proposed antenna with optimized geometry is shown in Fig. 5. The antenna presents a triple frequency band property, i.e., the first one ranging from 3.8GHz to 4GHz, the second one ranging from 4.9GHz to 6.31GHz, and the third one ranging from 7.35GHz to 7.5GHz. The simulated radiation patterns of the

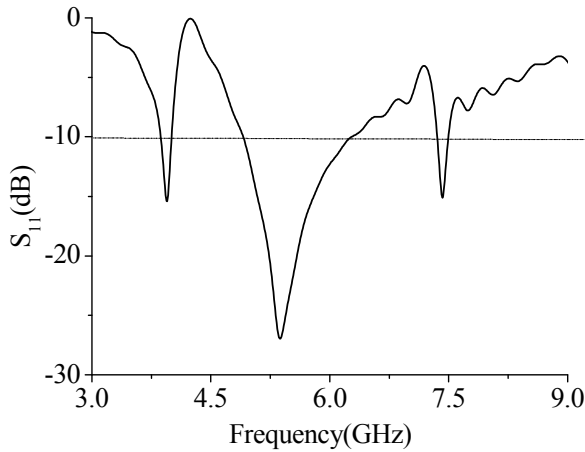


Fig. 5. Optimized return loss  $S_{11}$  of the proposed triple-band antenna

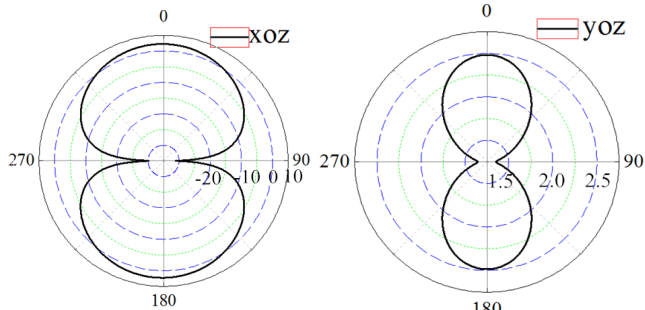


Fig. 6. Radiation patterns of triple-band antenna ( $f=3.95$ GHz)

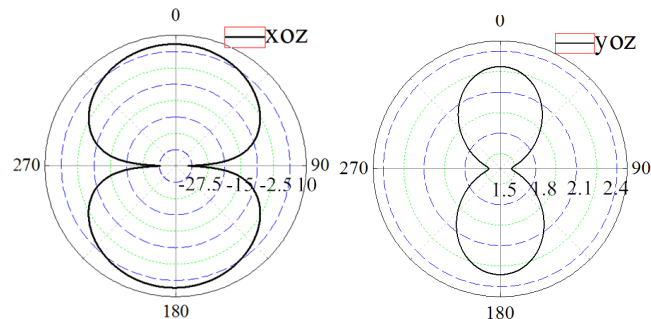


Fig. 7. Radiation patterns of triple-band antenna ( $f=5.4$ GHz)

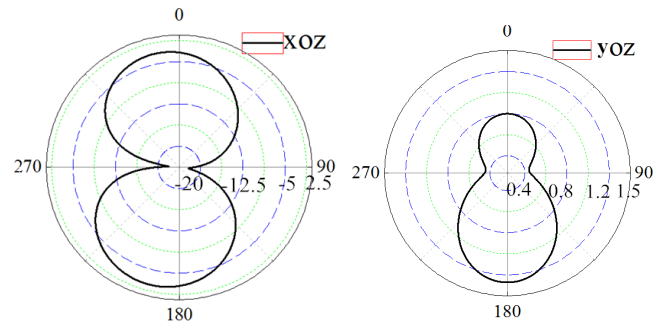


Fig. 8. Radiation patterns of triple-band antenna ( $f=7.4$ GHz)

proposed triple-band antenna at 3.95GHz, 5.4GHz, and 7.4GHz are plotted in Fig. 6, Fig. 7, and Fig. 8. The simulated gain of different frequency bands are 2.5dB, 2.3dB, and 1.3dB. The cross-polar levels are about 50dB smaller than the co-polar ones. It can be observed that in the first two operating frequency bands the antenna, i.e., the CSRR radiator, behaves similarly as a quarter-wave monopole. At the third operating frequency band, the main lobe is along the  $-z$ -direction due to the non-symmetric position of the LHTL to the square patch.

#### IV. CONCLUSION

A CPW-fed triple-band compact antenna based on CSRR and LHTL is presented in this paper. Simulation results show that the antenna can operate at 3.95GHz, 5.4GHz, and 7.4GHz with acceptable radiation properties, which makes it a good candidate for indoor communication applications. Further experimental results will be supplemented to the conference presentation to consolidate our simulation results.

#### ACKNOWLEDGMENT

This work was supported by National Natural Science Foundation of China under Grant No. 61301013. C. Liu and S. Xiao contributed equally to this work.

#### REFERENCES

- [1] K. Saurav, and D.S arkar, "Dual-Band Circularly Polarized Cavity-Backed Crossed-Dipole Antennas," *IEEE Trans. Antennas Propag.*, vol. 14, pp. 52-55, May 2014.
- [2] S. X. Ta, I. Park, and R. W. Ziolkowski, "Dual-band wide-beam crossed asymmetric dipole antenna for GPS application," *Electron. Lett.*, vol. 48, no. 25, pp. 1580-1581, Dec 2012.
- [3] K. Saurav, D. Sarkar, and K. V. Srivastava, "Dual polarized dual band patch antenna loaded with modified mushroom unit cell," *IEEE Antennas Wireless Propag. Lett.*, vol. 13, pp. 1357-1360, 2014.
- [4] K. Saurav, D. Sarkar, and K. V. Srivastava, "CRLH unit-cell loaded multi-band printed dipole antenna," *IEEE Antennas Wireless Propag. Lett.*, vol. 13, pp. 852-855, 2014.
- [5] F. Martinez, V. Posadas, L. Munoz, and D. Vargas, "Multi-frequency and dual-mode patch antennas partially filled with left-handed structures," *IEEE Trans. Antennas Propag.*, vol. 56, pp. 2527-2539, 2008.
- [6] P. Jin and R. Ziolkowski, "Multi-frequency, linear and circular polarized, metamaterial-inspired near-field resonant parasitic antennas," *IEEE Trans. Antennas Propag.*, vol. 59, no. 5, pp. 1446-1459, May. 2011.
- [7] Y. Dong and T. Itoh, "Miniaturized substrate integrated waveguide slot antennas based on negative order resonance," *IEEE Trans. Antennas Propag.*, vol. 58, no. 12, pp. 3856-3864, Dec. 2010.